EMBO reports

scientific report

# The oncometabolite 2-hydroxyglutarate inhibits histone lysine demethylases

*Rasheduzzaman Chowdhury[1], Kar Kheng Yeoh[1]*, Ya-Min Tian[2]*, Lars Hillringhaus[1], Eleanor A. Bagg[1], Nathan R. Rose[1], Ivanhoe K.H. Leung[1], Xuan S. Li[3], Esther C.Y. Woon[1], Ming Yang[1], Michael A. McDonough[1], Oliver N. King[1], Ian J. Clifton[1], Robert J. Klose[3], Timothy D.W. Claridge[1], Peter J. Ratcliffe[2], Christopher J. Schofield[1+] & Akane Kawamura[1++]*

[1]Chemistry Research Laboratory, Department of Chemistry, [2]Henry Wellcome Building for Molecular Physiology, Department of Clinical Medicine, and [3]Epigenetic Regulation of Chromatin Function Group, Department of Biochemistry, University of Oxford, Oxford, UK

**Mutations in isocitrate dehydrogenases (IDHs) have a gain-of-function effect leading to *R*(−)-2-hydroxyglutarate (*R*-2HG) accumulation. By using biochemical, structural and cellular assays, we show that either or both *R*- and *S*-2HG inhibit 2-oxoglutarate (2OG)-dependent oxygenases with varying potencies. Half-maximal inhibitory concentration ($IC_{50}$) values for the *R*-form of 2HG varied from approximately 25 μM for the histone $N^{\varepsilon}$-lysine demethylase JMJD2A to more than 5 mM for the hypoxia-inducible factor (HIF) prolyl hydroxylase. The results indicate that candidate oncogenic pathways in IDH-associated malignancy should include those that are regulated by other 2OG oxygenases than HIF hydroxylases, in particular those involving the regulation of histone methylation.**

Keywords: isocitrate dehydrogenase; 2-hydroxyglutarate; 2-oxoglutarate; oxygenases; hypoxia-inducible factor

EMBO *reports* (2011) **12**, 463–469. doi:10.1038/embor.2011.43

## INTRODUCTION

Heterozygous mutations in either of the two isoforms of the Krebs-cycle enzyme isocitrate dehydrogenase (IDH1/2) occur with a high prevalence in glioma, malignant glioblastoma and acute myeloid leukaemia (Dang *et al*, 2010; Reitman & Yan, 2010). The IDH mutations occur at substrate-binding arginine residues (Arg 132 in IDH1; Arg 140 and Arg 172 in IDH2) and inactivate IDH for conversion of isocitrate to 2-oxoglutarate (2OG; Zhao *et al*, 2009). However, they also cause a gain of function comprising catalysis of 2OG to the *R*-enantiomer of 2-hydroxyglutarate (*R*-2HG; Dang *et al*, 2009; Gross *et al*, 2010; Ward *et al*, 2010). The accumulation of *R*-2HG (to more than 10 mM in some cases) is associated with mutations of this type in both malignant glioblastoma and acute myeloid leukaemia, leading to the proposal that *R*-2HG is an 'oncometabolite'.

Increased L(*S*)-2HG or D(*R*)-2HG levels are also caused by germline mutations in L- or D-2-HG dehydrogenases, with excess *S*-2HG being correlated with an increased risk of brain tumour. *R*-2HG aciduria results in a more severe clinical manifestation than *S*-2HG aciduria, possibly precluding observation of tumours (Struys, 2006; Dang *et al*, 2010).

In some tumours, elevated levels of the Krebs-cycle intermediates succinate and fumarate result from mutations in succinate dehydrogenase and fumarate hydratase (Kaelin, 2009), which are proposed to stimulate the hypoxia-inducible factor (HIF)-mediated response. HIF target genes encode proteins that enable tumour growth, including vascular endothelial growth factor (Semenza, 2010). The HIF hydroxylases function as negative regulators of HIF-mediated transcription (Isaacs *et al*, 2005; Selak *et al*, 2005; Hewitson *et al*, 2007); thus, increased levels of succinate and fumarate are thought to promote tumour growth by inhibition of the HIF hydroxylases.

The HIF hydroxylases are Fe(II)- and 2OG-dependent oxygenases that produce succinate and $CO_2$ as coproducts; the HIF prolyl hydroxylases (PHD/EGLN enzymes) signal for HIF degradation, whereas factor inhibiting-HIF (FIH) is an asparaginyl hydroxylase that reduces HIF activity (Kaelin & Ratcliffe, 2008). Overexpression of IDH1 Arg 132 mutants results in elevated HIFα levels (Zhao *et al*, 2009). Other 2OG oxygenases are associated with cancer, including the JmjC histone demethylases (Varier & Timmers, 2010). This raises the question of whether 2HG inhibits 2OG oxygenases in a pathophysiologically relevant

[1]Chemistry Research Laboratory, Department of Chemistry, University of Oxford, Mansfield Road, Oxford OX1 3TA, UK
[2]Henry Wellcome Building for Molecular Physiology, Department of Clinical Medicine, University of Oxford, Roosevelt Drive, Oxford OX3 7BN, UK
[3]Epigenetic Regulation of Chromatin Function Group, Department of Biochemistry, University of Oxford, South Parks Road, Oxford OX1 3QU, UK
*These authors contributed equally to this work
[+]Corresponding author. Tel: +44 1865 275625; Fax: +44 1865 275674; E-mail: christopher.schofield@chem.ox.ac.uk
[++]Corresponding author. Tel: +44 1865 275631; Fax: +44 1865 275674; E-mail: akane.kawamura@chem.ox.ac.uk

**Received 27 October 2010; revised 21 February 2011; accepted 22 February 2011; published online 1 April 2011**

manner (Dang *et al*, 2010; Kaelin & Thompson, 2010). We report biochemical, structural and cellular studies showing that both *R*- and *S*-2HG inhibit 2OG oxygenases, but with different potencies. The results indicate that 2HG is a relatively poor inhibitor of the HIF hydroxylases in comparison to the 2OG-dependent histone lysyl demethylases, suggesting that candidate oncogenic pathways involving 2HG elevation might involve chromatin modifications.

## RESULTS

First, we investigated whether *R*- or *S*-2HG inhibit representative human 2OG oxygenases with the following roles: (i) HIF prolyl (PHD2/EGLN1) and asparaginyl (FIH) hydroxylation; (ii) fatty-acid metabolism (γ-butyrobetaine hydroxylase 1, BBOX1); (iii) histone demethylation (JMJD2A, JMJD2C and JHDM1A/FBXL11); and (iv) DNA demethylation activity (AlkB homologue 2, ABH2; Table 1; Fig 1). When using a 2OG concentration at or close to the $K_m$ (2OG) values for the individual enzymes, the half-maximal inhibitory concentration ($IC_{50}$) values for the *R*-/*S*-2HG ranged from approximately 25 μM to more than 10 mM. We used *N*-oxalylglycine (NOG), an unreactive 2OG analogue, for comparison. Of the two 2HG enantiomers, the *S*-form was the more-potent inhibitor. For *R*-2HG, the most significant inhibition was of JMJD2A, for which the $IC_{50}$ (24 μM) was similar to that observed for NOG (17 μM). By contrast, inhibition of PHD2 and BBOX1 by *R*-2HG was weak, with $IC_{50}$ values of approximately 7 and 13 mM, respectively, consistent with previous work with the PHDs (Mole *et al*, 2003).

The lack of a substantial increase in $IC_{50}$ values at higher (10-fold) iron concentrations (for JMJD2A and BBOX-1), and different values for the two enantiomers imply that the mode of inhibition is not predominantly iron sequestration (Table 1). We investigated whether *R*- or *S*-2HG is oxidized to 2OG by PHD2 and FIH; in our standard conditions, we did not find conversion of 2HG to 2OG by NMR analysis (data not shown). Neither *R*- nor *S*-2HG was a cosubstrate for PHD2 (supplementary Fig S1 online). Although care must be taken in comparing $IC_{50}$ values determined with different assay conditions for the various oxygenases, these results show that both *R*- and *S*-2HG inhibit the 2OG oxygenases, but with different potencies. The weak inhibition of the HIF hydroxylases suggests that the pathological effects of 2HG are probably not, at least predominantly, mediated by direct inhibition of HIF hydroxylases.

We then investigated the structural basis of oxygenase inhibition by 2HG. Structures of FIH and JMJD2A with *R*- or *S*-2HG show that both can bind to the active site iron, or surrogate nickel, in a bidentate manner (Fig 2). The JMJD2A.2HG structures were obtained with a histone H3K36me3 substrate fragment, which bound similarly to previously reported structures (Chen *et al*, 2006; Couture *et al*, 2007; Ng *et al*, 2007). Similarly to 2OG and NOG (Elkins *et al*, 2003; Ng *et al*, 2007), both *R*- and *S*-2HG coordinate the metal with the 2-hydroxyl group *trans* to $D201^{FIH}$/$E190^{JMJD2A}$ and one oxygen of the C1-carboxylate *trans* to $H199^{FIH}$/$H188^{JMJD2A}$ (Fig 2A,B,D,E). The other oxygen of the 2HG C1-carboxylate is positioned to hydrogen bond to Nδ2 of $N205^{FIH}$ (Fig 2A,B) or to Oγ of $S288^{JMJD2A}$ (Fig 2D,E); the 2HG C5-carboxylate is positioned to hydrogen bond to $K214^{FIH}$ Nζ, $Y145^{FIH}$ OH and $T196^{FIH}$ Oγ1 (Fig 2A,B) and to $K206^{JMJD2A}$ Nζ and $Y132^{JMJD2A}$ OH (Fig 2D,E), as observed for the 2HG C5-carboxylate. In FIH, the remaining metal coordination site is probably occupied by a glycerol molecule derived from the cryoprotectant solution (not shown in Fig 2A,B) and by water in JMJD2A structures (Fig 2D,E). Overall, the crystallographic analyses indicte that, similarly to succinate and fumarate (Fig 2C,F; Hewitson *et al*, 2007), both *R*- and *S*-2HG have the potential to bind to the active site Fe(II) and compete with 2OG for binding. To test this proposal, we performed further kinetic analyses. These indicate that, although NOG is a 2OG competitor, inhibition of JMJD2A by *R*-/*S*-2HG might be more complex; *R*-2HG demonstrated mixed-mode inhibition kinetics and—within the concentration ranges for which we could reliably obtain data—the *S*-2HG seemed to give uncompetitive kinetics with respect to 2OG (supplementary Fig S2 online; at higher *S*-2HG concentrations, inhibition by *S*-2HG might be mixed, but we were unable to obtain reliable data because of the low level of turnover at high *S*-2HG concentrations). A possible explanation for the results of our combined crystallographic and kinetic analyses is that, at least for *R*-2HG, the inhibitor can bind to both the enzyme.Fe(II) complex competing with 2OG and the enzyme.Fe(II).2OG complex. No additional 2HG binding was observed in the JMJD2A crystal structures. However, support for this idea comes from the observation that, at sufficiently high concentrations, 2OG itself inhibits some 2OG oxygenases—including AlkB (Welford *et al*, 2003), JMJD2A and FBXL11 (unpublished data)—and from crystallographic analyses indicating the potential for coordination of two organic molecules at the active-site metal; glycerol to the FIH.Fe(II).2HG complexes and with inhibitor studies on FIH (Conejo-Garcia *et al*, 2010). Work on deacetoxycephalosporin C synthase–succinate complexes also suggests that binding modes of diacids different to that normally observed for 2OG can also occur (Lee *et al*, 2001).

We then investigated inhibition of 2OG oxygenases by 2HG in cells (Fig 3), by testing JMJD2A because its $IC_{50}$ values were lowest (Fig 3A,B). A cell-penetrating ester form of *R*-/*S*-2HG

**Table 1** | Inhibition of human 2OG oxygenases by *R*- and *S*-2HG

| Enzyme | $IC_{50}$ ± s.e.m. (μM) | | |
|---|---|---|---|
| | ***R*-2HG** | ***S*-2HG** | **NOG** |
| FIH | 1,500 ± 400* | 189 ± 34 | 46 ± 8 |
| PHD2 | 7,300 ± 3,300* | 419 ± 150 | 0.8 ± 0.2 |
| JMJD2A | 24 ± 2 (*17 ± 4*) | 26 ± 3 (*33 ± 5*) | 17 ± 2 (*20 ± 3*) |
| JMJD2C | 79 ± 7 | 97 ± 24 | 14 ± 3 |
| FBXL11 | 106 ± 22 | 48 ± 15 | 252 ± 50 |
| ABH2 | 424 ± 77 | 150 ± 20 | 10 ± 2 |
| BBOX1 | 13,200 ± 1,100 | 142 ± 30 (*96 ± 10*) | 19 ± 2 |

Substrates used in the assays for JMJD2A/JMJD2C, FBXL11, BBOX1, PHD2, FIH and ABH2 were histone H3 fragment substrates H3(7–14)K9me$_3$ and H3(30–41)K36me$_2$, γ-butyrobetaine, HIF1αCODD (residues 556–574), HIF1αCAD (residues 786–826) and GCXAGGTCCCGTAGTGCG, where X is 1-methyladenylate, respectively. See Fig 1 for dose–response curves and supplementary Table S1 online for the standard assay conditions used for the individual enzymes. Italicized $IC_{50}$ values in parentheses were determined at 10-fold higher Fe(II) concentration than the standard assay conditions.
*Partial dose–response curves.
ABH2, AlkB homologue 2; BBOX1, γ-butyrobetaine hydroxylase 1; FIH, factor inhibiting-hypoxia-inducible factor; HIF, hypoxia-inducible factor; NOG, *N*-oxalylglycine; 2OG, 2-oxoglutarate; PHD2, prolyl hydroxylase 2; *R*-2HG, *R*-enantiomer of 2-hydroxyglutarate; $IC_{50}$, half-maximal inhibitory concentration.

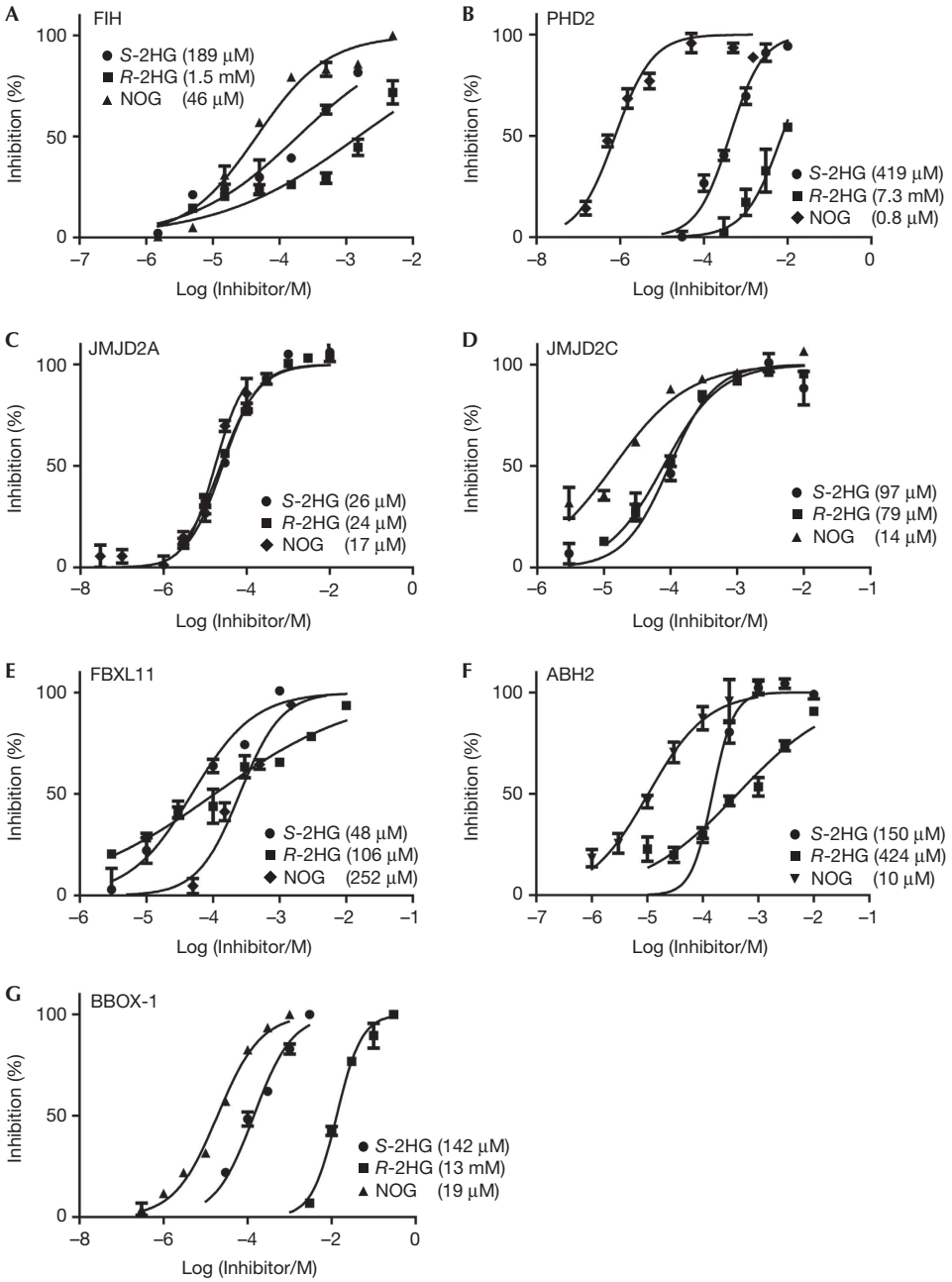


**Fig 1** | Inhibition of recombinant forms of 2OG oxygenases by *R*-/*S*-2HG and *N*-oxalylglycine. (**A**) Inhibition of FIH as assessed by measuring hydroxylation of HIF1αCAD using a MALDI–TOF–MS assay. (**B**) Inhibition of PHD2 as assessed by measuring hydroxylation of HIF1αCODD using a MALDI–TOF–MS assay. Inhibition of (**C**) JMJD2A, (**D**) JMJD2C, (**E**) FBXL11 and (**F**) ABH2 by *R*-, *S*-2HG and NOG, as assessed by using formaldehyde dehydrogenase-based assay. (**G**) Inhibition of BBOX1 by *S*-2HG and *R*-2HG as compared with the standard NOG by NMR. All assays were performed in triplicate and are shown as averages with s.e.m. $IC_{50}$ values were calculated using log(inhibitor) compared with normalized response (variable slope), using the program Prism, and are given in parentheses. The assay conditions for each enzyme are described in supplementary Table S1 online. ABH2, AlkB homologue 2; BBOX1, γ-butyrobetaine hydroxylase 1; FIH, factor inhibiting-hypoxia-inducible factor; HIF, hypoxia-inducible factor; 2OG, 2-oxoglutarate; PHD2, prolyl hydroxylase 2; *R*-2HG, *R*-enantiomer of 2-hydroxyglutarate; $IC_{50}$, half-maximal inhibitory concentration; MALDI–TOF–MS, matrix-assisted laser desorption/ionization–time of flight–mass spectrometry; NOG, *N*-oxalylglycine.

was added to HeLa cells transfected with JMJD2A (Fig 3A). Dimethyloxalylglycine—a cell-penetrating derivative of NOG—was used as a positive control. At high concentrations (8 × 5 mM or 10-mM additions at 30-min intervals), both enantiomers inhibited JMJD2A in a dose-dependent manner (Fig 3B); consistent with the *in vitro* data, the extent of inhibition was similar for

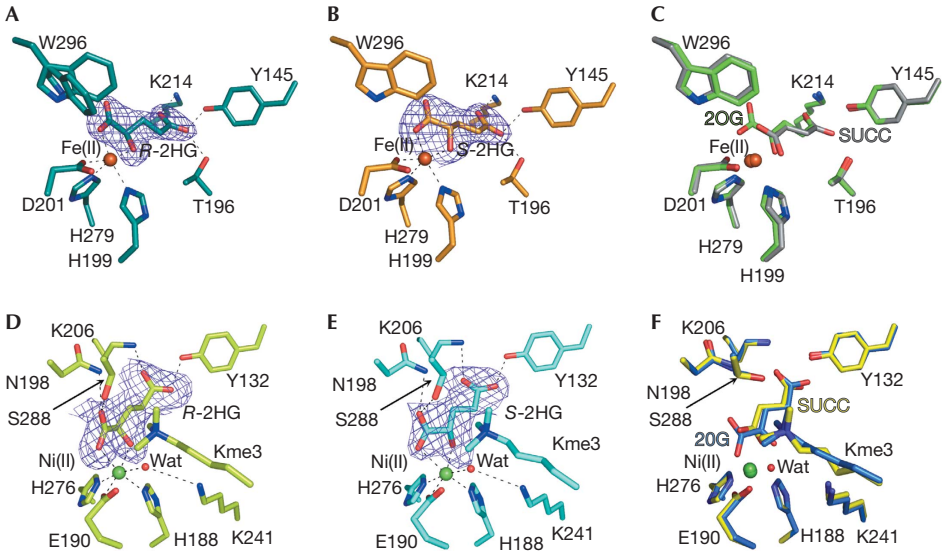


**Fig 2** | Crystal structures of FIH and JMJD2A in complex with *R*- and *S*-2HG indicate binding of 2HG to the 2OG-binding site. FIH/JMJD2A folds were similar to those reported (RMSD for Cα ⩽ 0.3 Å for monomers). Dotted lines indicate apparent hydrogen bonds and polar interactions. Data collection and refinement statistics are given in supplementary Table S2 online. (**A**) View of the FIH.Fe(II).*R*-2HG complex showing the *Fo*–*Fc* omit map (contoured to 6 σ) for *R*-2HG. Notably, the side chain of Trp 296$^{FIH}$, which is involved in substrate binding (Elkins *et al*, 2003), has two conformations. (**B**) FIH.Fe(II).*S*-2HG structure showing the *Fo*–*Fc* omit map contoured to 6 σ around *S*-2HG. (**C**) Overlay of views from structures of FIH in complex with 2OG or succinate. (**D**) View from the active site of the JMJD2A.Ni(II).*R*-2HG.H3K36me$_3$ structure showing the *Fo*–*Fc* omit map contoured to 3.5 σ around *R*-2HG; Kme3 = N$^{\varepsilon}$-trimethylated lysine substrate residue; Ni(II) substitute for Fe(II). (**E**) JMJD2A.Ni(II).*S*-2HG.H3K36me$_3$ structure showing the *Fo*–*Fc* omit map contoured to 3.5 σ around *S*-2HG. (**F**) Overlay of views from structures of JMJD2A in complex with 2OG or succinate. (**D**–**F**) Both *R*-/*S*-2HG induce a rotation of approximately 100° (relative to other JMJD2A structures) about Cα-Cβ of the Ser 288$^{JMJD2A}$ side chain such that it is positioned to hydrogen bond to 2HG (Ser Oγ-*R*/*S*-2HG O2; 2.8/3.1 Å). Ser 288$^{JMJD2A}$ is proposed to be involved in substrate recognition and a determinant of the specificity of JMJD2 for different methylation states (Chen *et al*, 2006). FIH, factor inhibiting-hypoxia-inducible factor; 2OG, 2-oxoglutarate; *R*-2HG, *R*-enantiomer of 2-hydroxyglutarate; RMSD, root mean square deviation.

*R*-/S-2HG. We then tested for HIF hydroxylation inhibition using hydroxyl-residue antibodies and von Hippel Lindau protein (VHL)-defective renal cell carcinoma (RCC4) cells to enable simultaneous measurement of Pro- and Asn-hydroxylation (Fig 3C,D). Consistent with *in vitro* data, we observed a clear reduction in HIF1α Asn-hydroxylation, that was greater with *S*- than *R*-2HG. In contrast to these results and consistent with the *in vitro* data, we observed no *R*-2HG and only minimal *S*-2HG inhibition of Pro-hydroxylation, when using the same doses at which JMJD2A was inhibited (exposure to higher 2HG doses was toxic).

These results suggest that 2HG—and in particular the *R*-enantiomer produced by IDH1 mutants (Dang *et al*, 2009)—is probably an ineffective inhibitor of HIF Pro-hydroxylation, and predict that it would be relatively ineffective in inducing HIF1α. To test this, stable RCC4 transfectants re-expressing wild-type VHL (RCC4/VHLHA) and other VHL-competent cell lines (Hep3B/MCF7 cells) were exposed to several 10-mM additions or a single 20-mM addition of the methyl esters of *R*-/*S*-2HG. Neither dose of *R*-2HG induced HIF1α. Modest induction was observed with *S*-2HG (Fig 3E). As both the *in vitro* and cell studies indicate that HIF Asn-hydroxylation is more 2HG-sensitive than Pro-hydroxylation, we suggested that HIF1α induced by 2HG would not be hydroxylated at the site of Asn-hydroxylation in the C-terminal activation domain. We found this is the case (Fig 3F).

## DISCUSSION

Overall, our results demonstrate that *R*- and *S*-2HG have the potential to inhibit a range of human 2OG oxygenases, thereby suggesting one mechanism by which elevated 2HG levels might promote oncogenesis. Although the inhibition potencies are generally weak, we observe broad concordance between the *in vitro* and *in vivo* results (Table 1; Figs 1 and 3). As production of 2HG by IDH mutations is stereospecific (Dang *et al*, 2009; Ward *et al*, 2010), the specificity of inhibition by the 2HG enantiomers is relevant to their potential as mediators of oncogenic pathways. For most of the 2OG oxygenases tested *in vitro*, *S*-2HG was more potent than *R*-2HG (Table 1). Only with the histone N$^{\varepsilon}$-methyl lysine demethylases JMJD2A/C were both enantiomers of similar potency, and of the enzymes tested, JMJD2A was the only one for which *R*-2HG showed similar potency to NOG, a 'generic' 2OG oxygenase inhibitor. Interestingly, inactivating mutations and/or reduced expression of JmjC histone demethylases including JARID1C (Dalgliesh *et al*, 2010), UTX (van Haaften *et al*, 2009) and JHDM1B/FBXL10 (Frescas *et al*, 2007), occur in RCCs, multiple myeloma, glioblastoma multiforme and several other cancers. Given the similarity of JMJD2A to some other JmjC histone demethylases, it is likely that *R*-2HG will inhibit at least some other demethylases with a similar or greater potency than JMJD2A. Our results therefore support the candidacy of one or more of these enzymes as targets for pathologically relevant 2HG

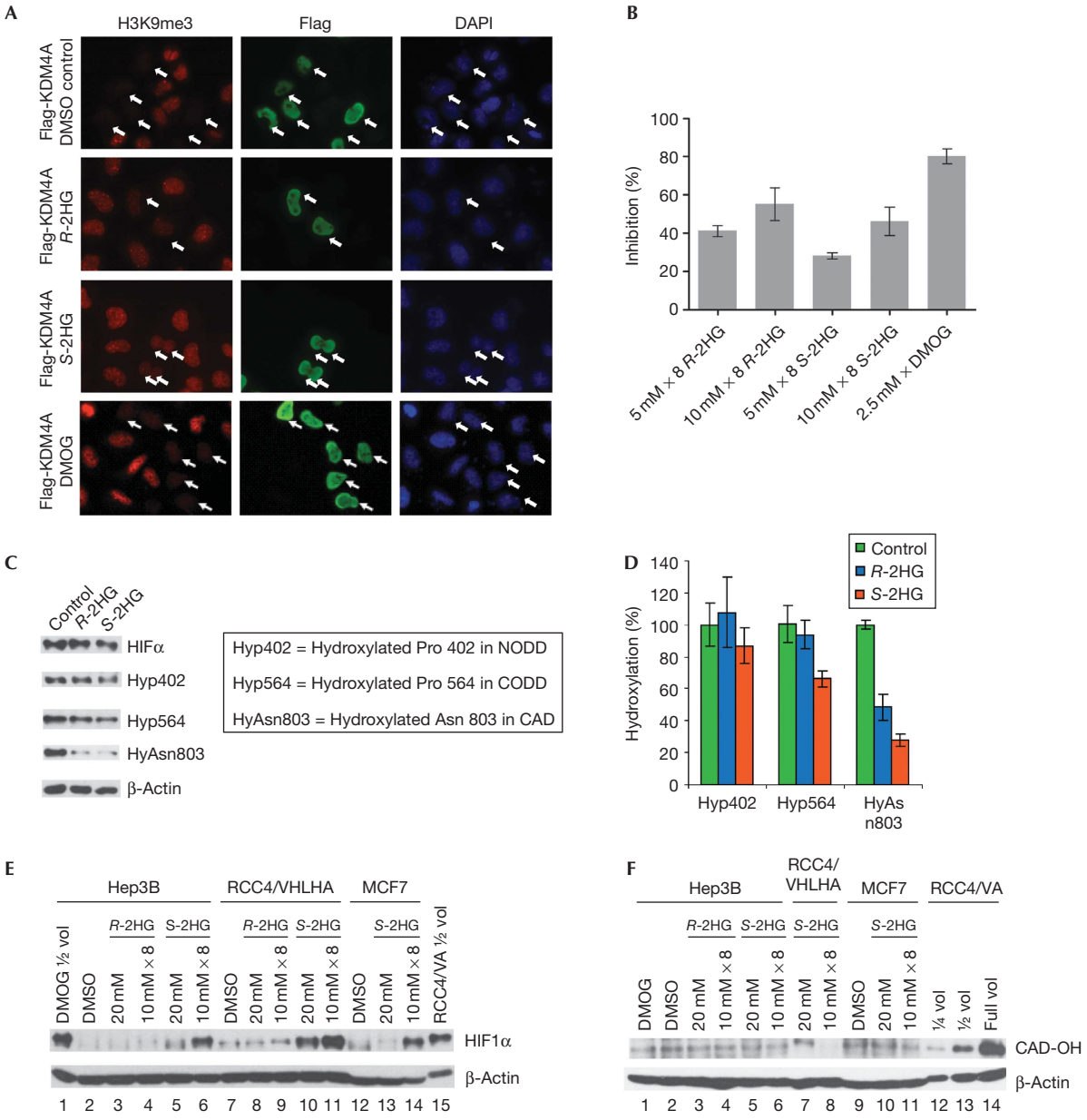


**Fig 3** | Inhibition of histone demethylases and HIF hydroxylases by *R*- and *S*-2HG. (**A**,**B**) Inhibition of JMJD2A activity in HeLa cells, as shown by immunofluorescence studies. JMJD2A was expressed as an *N*-terminally Flag-tagged protein. The results for DMOG, a cell-penetrating form of the 'generic' 2OG oxygenase inhibitor NOG, are shown for comparison. (**A**) Indirect immunofluorescence analyses using antibodies against $H3K9me_3$ (left panels) or Flag (middle panels) were used to analyse the inhibition of ectopically expressed JMJD2A. DAPI staining (right panels) indicates location of nuclei. Rows represent control (0.5% DMSO), *R*-/*S*-2HG- and DMOG-treated cells. White arrows in the left and right panels indicate nuclei in which JMJD2A is overexpressed. Higher levels of $H3K9me_3$ were detected in both *R*- and *S*-2HG-treated cells, indicating inhibition of JMJD2A, whereas the control shows only a level of $H3K9me_3$ in nuclei in which JMJD2A is overexpressed. (**B**) Percentage inhibition of JMJD2A activity, using addition of doses of *R*- and *S*-2HG in their dimethyl ester forms (5 or 10 mM × 8); error bars represent standard error ($n > 50$). (**C**,**D**) Effect of *R*-/*S*-2HG on HIF1α hydroxylation in VHL-defective RCC4/VA cells. (**C**) Immunoblots of protein extracts from RCC4 cells treated for 4 h with *R*- and *S*-2HG compared with a DMSO-treated control. The compounds were added using the same dosing regime (10 mM × 8) as was used for the JMJD2A cell-work in their dimethyl ester forms. Signals of total HIF1α and hydroxylated NODD, CODD and CAD were analysed. (**D**) Quantification of data from (**C**) by densitometry; band intensities were normalized to HIF1α signals. Vertical bars represent standard errors ($n > 3$). (**E**) Effect of *R*-/*S*-2HG on HIF1α protein levels in human hepatoma (Hep3B), renal (RCC4/VHLHA, overexpressing haemagglutinin-tagged VHL) and breast cancer (MCF7) cells. (**F**) Immunoblot analyses of HIF1α CAD hydroxylation of selected samples from (**E**). DMOG, dimethyloxalylglycine; HIF, hypoxia-inducible factor; NOG, *N*-oxalylglycine; RCC, renal cell carcinoma; *R*-2HG, *R*-enantiomer of 2-hydroxyglutarate; 2OG, 2-oxoglutarate.

inhibition. However, they by no means exclude other 2OG oxygenases or other mechanisms of 2HG-mediated tumour promotion from a role in oncogenesis.

The high concentrations of *R*-2HG (more than 10 mM) that have been observed in malignant brain tumours and leukaemias (Dang *et al*, 2009; Gross *et al*, 2010; Ward *et al*, 2010), might be sufficient to inhibit even the less-susceptible 2OG oxygenases. Nevertheless, PHD2 is poorly inhibited *in vitro* by *R*-2HG (Fig 1; Table 1), and we were unable to demonstrate inhibition of the PHDs sufficient to substantially upregulate HIF in cells (Fig 3C–E). HIF is stabilized in IDH-associated gliomas; this has been proposed to be a consequence of intracellular depletion of 2OG following IDH loss of function (Zhao *et al*, 2009). It is possible that the depleted 2OG levels might synergize with *R*-2HG, or that IDH mutations perturb the $NADP^+/NADPH + H^+$ ratio, causing redox stress (Dang *et al*, 2010), inactivating the HIF hydroxylases and upregulating HIF by an unknown mechanism.

In conclusion, our findings argue against upregulation of HIF through PHD inhibition by 2HG being the major factor in IDH mutation-associated oncogenesis. However, they show that elevated 2HG levels might regulate gene expression by inhibition of 2OG-dependent chromatin-modifying enzymes, including the JmjC histone demethylases. Furthermore, they demonstrate that accumulation of *R*-2HG has the potential to modulate the transcriptional activity of the HIF pathway by acting on Asn-hydroxylation. Inhibition of Asn-hydroxylation in the C-terminal transactivation domain of HIFα polypeptides might be predicted to enhance transcriptional activity through the recruitment of p300/CBP coactivators to the C-terminal activation domain (Kaelin & Ratcliffe, 2008). As HIF transcriptional target genes are differently dependent on the activity of this domain, such an action might affect hypoxia pathways.

## METHODS

Details of materials used, syntheses, recombinant protein production, additional assay and crystallography are given in supplementary information online.

**Biochemical assays.** (See supplementary Table S1 online for assay conditions). Assays using mass spectrometry involved incubation of the enzyme in the presence of Fe(II), 2OG, ascorbate and peptide. Product formation was assessed by using matrix-assisted laser desorption/ionization–time of flight–mass spectroscopy assay (Hewitson *et al*, 2007; Rose *et al*, 2008; Chowdhury *et al*, 2009). JMJD2A, JMJD2C, FBXL11 and ABH2 inhibition were assessed using a formaldehyde dehydrogenase-coupled assay (Couture *et al*, 2007; Roy & Bhagwat, 2007; Rose *et al*, 2008).

**Histone demethylase assays.** HeLa cells grown in Dulbecco's modified eagle's medium containing 10% fetal bovine serum and penicillin/streptomycin were divided into six-well plates and transfected with 2 μg Flag-JMJD2A plasmid per well using Fugene HD (Roche). Compounds were added 5 h after transfection (5- and 10-mM *R*- and *S*-2HG was added at 30-min intervals for 4 h ( × 8); 2.5-mM dimethyloxalyl glycine was added once). Cells were fixed 9 h after transfection (20 min in 4% formaldehyde), washed twice with PBS, then permeabilized for 10 min (0.5% Triton X-100/PBS). Permeabilized cells were washed twice in PBS, placed in 3% BSA/PBS (30 min) and then washed twice with PBS. Immunostaining using α-$H3K9me_3$ (1:500; Ab8898, Abcam) and data analysis was carried out as described previously (King *et al*, 2010). Data were normalized by setting DMSO-treated JMJD2A-transfected cells to 100% activity and a catalytically inactive JMJD2A H188A mutant to 0% activity.

**HIF hydroxylase assays.** Both VHL-defective (RCCs with an empty vector RCC4/VA) and VHL-competent cells, i.e. human heptoma Hep3B, breast cancer MCF7 and RCC4/VHLHA (RCC4 stably transfected with *C*-haemagglutinin-tagged wild-type VHL), were used. In brief (details of this assay will be reported elsewhere), cells were treated with DMSO (control) or *R*-/*S*-2HG dimethyl esters (4 h). Compounds were added at concentrations of 20 mM ( × 1) or 10 mM ( × 8, at 30-min intervals). Cell extracts were probed with antibodies for hydroxy-Pro 402 (NODD-OH), hydroxy-Pro564 (CODD-OH) and hydroxy Asn 803 (CAD-OH). HIF1α band intensities were used to normalize hydroxylation signals. Antibodies for HIF1α, NODD-OH, CODD-OH and β-actin/horseradish peroxidase were obtained from BD Transduction Laboratories, Millipore Biosciences, New England Biolabs and Abcam, respectively. The CAD-OH antibody was a gift from Dr S.H. Lee (Lee *et al*, 2008).

**Supplementary information** is available at EMBO *reports* online (http://www.emboreports.org).

ACKNOWLEDGEMENTS

We thank the scientists of Diamond beamline I04, Oxford, UK for assistance.This work was funded by the Wellcome Trust, the Biotechnology and Biological Sciences Research Council, UK, the German Academic Exchange Service (L.H.), the Malaysian Government and Univerisiti Sains Malaysia (K.K.Y.).

*Author contributions:* R.C., A.K., I.K.H.L., C.J.S. and P.J.R conceived and designed the experiments. R.C., K.K.Y., Y.M.T., A.K., L.H., E.A.B., N.R.R., I.K.H.L., E.C.Y.W. and X.S.L performed the experiments. R.C., K.K.Y., Y.M.T., A.K., L.H., I.K.H.L., C.J.S. and P.J.R analysed the data. M.Y., O.N.K., M.A.M., I.J.C., R.J.K. and T.D.W.C contributed reagents, materials and analysis tools. R.C., A.K., P.J.R. and C.J.S wrote the paper.

CONFLICT OF INTEREST

The authors declare that they have no conflict of interest.

REFERENCES

Chen Z *et al* (2006) Structural insights into histone demethylation by JMJD2 family members. *Cell* **125:** 691–702

Chowdhury R, McDonough MA, Mecinovic J, Loenarz C, Flashman E, Hewitson KS, Domene C, Schofield CJ (2009) Structural basis for binding of hypoxia-inducible factor to the oxygen-sensing prolyl hydroxylases. *Structure* **17:** 981–989

Conejo-Garcia A, McDonough MA, Loenarz C, McNeill LA, Hewitson KS, Ge W, Lienard BM, Schofield CJ, Clifton IJ (2010) Structural basis for binding of cyclic 2-oxoglutarate analogues to factor-inhibiting hypoxia-inducible factor. *Bioorg Med Chem Lett* **20:** 6125–6128

Couture JF, Collazo E, Ortiz-Tello PA, Brunzelle JS, Trievel RC (2007) Specificity and mechanism of JMJD2A, a trimethyllysine-specific histone demethylase. *Nat Struct Mol Biol* **14:** 689–695

Dalgliesh GL *et al* (2010) Systematic sequencing of renal carcinoma reveals inactivation of histone modifying genes. *Nature* **463:** 360–363

Dang L *et al* (2009) Cancer-associated IDH1 mutations produce 2-hydroxyglutarate. *Nature* **462:** 739–744

Dang L, Jin S, Su SM (2010) IDH mutations in glioma and acute myeloid leukemia. *Trends Mol Med* **16:** 387–397

Elkins JM, Hewitson KS, McNeill LA, Seibel JF, Schlemminger I, Pugh CW, Ratcliffe PJ, Schofield CJ (2003) Structure of factor-inhibiting hypoxia-inducible factor (HIF) reveals mechanism of oxidative modification of HIF-1a. *J Biol Chem* **278:** 1802–1806

Frescas D, Guardavaccaro D, Bassermann F, Koyama-Nasu R, Pagano M (2007) JHDM1B/FBXL10 is a nucleolar protein that represses transcription of ribosomal RNA genes. *Nature* **450:** 309–313

Gross S *et al* (2010) Cancer-associated metabolite 2-hydroxyglutarate accumulates in acute myelogenous leukemia with isocitrate dehydrogenase 1 and 2 mutations. *J Exp Med* **207:** 339–344

Hewitson KS, Lienard BM, McDonough MA, Clifton IJ, Butler D, Soares AS, Oldham NJ, McNeill LA, Schofield CJ (2007) Structural and mechanistic studies on the inhibition of the hypoxia-inducible transcription factor hydroxylases by tricarboxylic acid cycle intermediates. *J Biol Chem* **282:** 3293–3301

Isaacs JS *et al* (2005) HIF overexpression correlates with biallelic loss of fumarate hydratase in renal cancer: novel role of fumarate in regulation of HIF stability. *Cancer Cell* **8:** 143–153

Kaelin WG Jr (2009) SDH5 mutations and familial paraganglioma: somewhere Warburg is smiling. *Cancer Cell* **16:** 180–182

Kaelin WG Jr, Ratcliffe PJ (2008) Oxygen sensing by metazoans: the central role of the HIF hydroxylase pathway. *Mol Cell* **30:** 393–402

Kaelin WG Jr, Thompson CB (2010) Q&A: Cancer: clues from cell metabolism. *Nature* **465:** 562–564

King ONF *et al* (2010) Quantitative high-throughput screening identifies 8-hydroxyquinolines as cell-active histone demethylase inhibitors. *PLoS ONE* **5:** e15535

Lee HJ, Lloyd MD, Harlos K, Clifton IJ, Baldwin JE, Schofield CJ (2001) Kinetic and crystallographic studies on deacetoxycephalosporin C synthase (DAOCS). *J Mol Biol* **308:** 937–948

Lee SH, Jeong Hee M, Eun Ah C, Ryu SE, Myung Kyu L (2008) Monoclonal antibody-based screening assay for factor inhibiting hypoxia-inducible factor inhibitors. *J Biomol Screen* **13:** 494–503

Mole DR, Schlemminger I, McNeill LA, Hewitson KS, Pugh CW, Ratcliffe PJ, Schofield CJ (2003) 2-oxoglutarate analogue inhibitors of HIF prolyl hydroxylase. *Bioorg Med Chem Lett* **13:** 2677–2680

Ng SS *et al* (2007) Crystal structures of histone demethylase JMJD2A reveal basis for substrate specificity. *Nature* **448:** 87–91

Reitman ZJ, Yan H (2010) Isocitrate dehydrogenase 1 and 2 mutations in cancer: alterations at a crossroads of cellular metabolism. *J Natl Cancer Inst* **102:** 932–941

Rose NR, Ng SS, Mecinovic J, Lienard BM, Bello SH, Sun Z, McDonough MA, Oppermann U, Schofield CJ (2008) Inhibitor scaffolds for 2-oxoglutarate-dependent histone lysine demethylases. *J Med Chem* **51:** 7053–7056

Roy TW, Bhagwat AS (2007) Kinetic studies of *Escherichia coli* AlkB using a new fluorescence-based assay for DNA demethylation. *Nucleic Acids Res* **35:** e147

Selak MA, Armour SM, MacKenzie ED, Boulahbel H, Watson DG, Mansfield KD, Pan Y, Simon MC, Thompson CB, Gottlieb E (2005) Succinate links TCA cycle dysfunction to oncogenesis by inhibiting HIF-α prolyl hydroxylase. *Cancer Cell* **7:** 77–85

Semenza GL (2010) Defining the role of hypoxia-inducible factor 1 in cancer biology and therapeutics. *Oncogene* **29:** 625–634

Struys EA (2006) D-2-Hydroxyglutaric aciduria: unravelling the biochemical pathway and the genetic defect. *J Inherit Metab Dis* **29:** 21–29

van Haaften G *et al* (2009) Somatic mutations of the histone H3K27 demethylase gene UTX in human cancer. *Nat Genet* **41:** 521–523

Varier RA, Timmers HT (2010) Histone lysine methylation and demethylation pathways in cancer. *Biochim Biophys Acta* **1815:** 75–89

Ward PS *et al* (2010) The common feature of leukemia-associated IDH1 and IDH2 mutations is a neomorphic enzyme activity converting a-ketoglutarate to 2-hydroxyglutarate. *Cancer Cell* **17:** 225–234

Welford RW, Schlemminger I, McNeill LA, Hewitson KS, Schofield CJ (2003) The selectivity and inhibition of AlkB. *J Biol Chem* **278:** 10157–10161

Zhao S *et al* (2009) Glioma-derived mutations in IDH1 dominantly inhibit IDH1 catalytic activity and induce HIF-1a. *Science* **324:** 261–265